JP2J.5 **PRELIMINARY STUDY ON THE STRUCTURES OF LINE-ECHO WAVE PATTERN OVER THE OCEAN IN THE SUBTROPICAL**

Chih-Hsien Wei* and Wen-Chau Lee
National Center for Atmospheric Research, Boulder, Colorado

1. INTRODUCTION

The lifecycle of bow echoes and their accompanying mesoscale convective vortices (MCV) was first proposed by Fujita (1981). An elongated echo evolves into a bow echo then evolves into MCV at the later stage of its lifecycle. Sometimes these systems are embedded in line echo wave pattern (LEWP) as part of a squall line or a mesoscale convective system (MCS). There were few observational studies on these systems until the Bow Echo and Mesoscale Convective Vortex Experiment (BAMEX 2003, Davis et al 2004). Previously, numerical simulations (e.g., Weisman 1992; Weisman and Davis 1998) have been the primary tools to study these systems. Although the Coriolis force have been attributed to the cyclonic asymmetry of these systems in the northern hemisphere (Skamarock et al.1994), Jorgensen et al (1997) documented such a system in the tropics where Coriolis force is weak In fact, Bow echo and MCV systems have rarely been observed in tropical and subtropical regions.

A MCS developed over the southern part of the Taiwan Strait on 7 June 2003 (Fig 1). The leading convection possessed a LEWP moved through southern Taiwan and subsequently evolved into bow segments and MCVs. The northern part of the system was observed by both Central Weather Bureau's operational Doppler radars located at Chiku (RCCG) and Kenting (RCKT). Dual-Doppler wind synthesis from both radars thus can deduce the kinematic structure of the system. Not only it was a unique observation on LEWP, in subtropical area, but it is the first dual-Doppler observation of such a mesoscale system in East Asian area over the ocean to date. This paper presents the evolution and structure of this bow echo and MCV system particularly on the northern end of the system residing in the dual-Doppler lobe

2. DATA SOURCES AND METHODOLOGY

The primary data come from the operational Doppler radars in Southern Taiwan (RCCG and RCKT). Both radars provided volume scans of the system at an interval of 8 to 10 min from 0116 to 0300 UTC 7 June 2003. The radar scans were not coordinated so there was up to 5 min differences in start times of

*Corresponding author address: Chih-Hsien Wei, National Center for Atmospheric Research, Boulder CO 80307-3000; e-mail: weic@ucar.edu

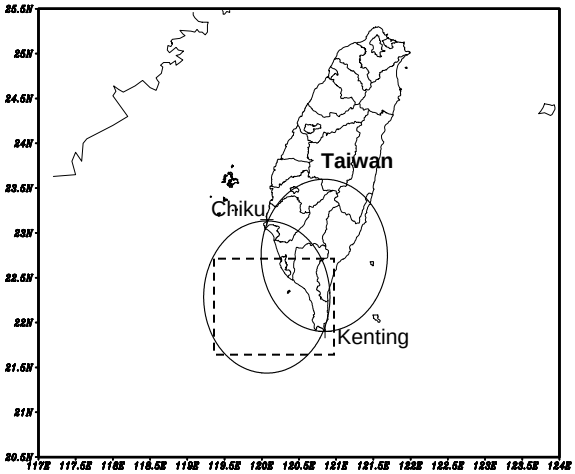

Fig. 1 Map for the domain of dual-Doppler analysis. The enclosed dashed area represents study region of this case.

corresponding radar volumes in the dual-Doppler radar synthesis. The Doppler radar data were edited in the NCAR SOLO software to remove non-meteorological returns (such as noise, ground clutter, blockage etc). The wind synthesis is performed using standard dual-Doppler routines and softwares (REORDER, Oye 1995, provided by NCAR/EOL and CEDRIC, Mohr et al. 1986, provided by NCAR/MMM). Conventional observations, such as synoptic weather analyses, soundings and mesonet, are also included in this study.

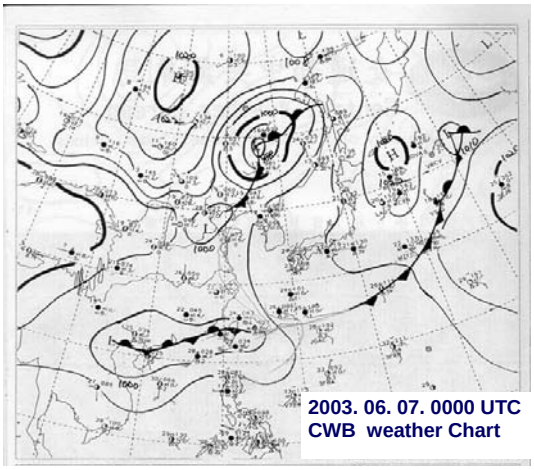

Fig. 2 Surface chart at 0000 UTC 7 June 2003.

3. SYNOPTIC AND MESOSCALE CONDITIONS

The stationary front existed in the region from northern Taiwan to southeastern coast of China at 0000

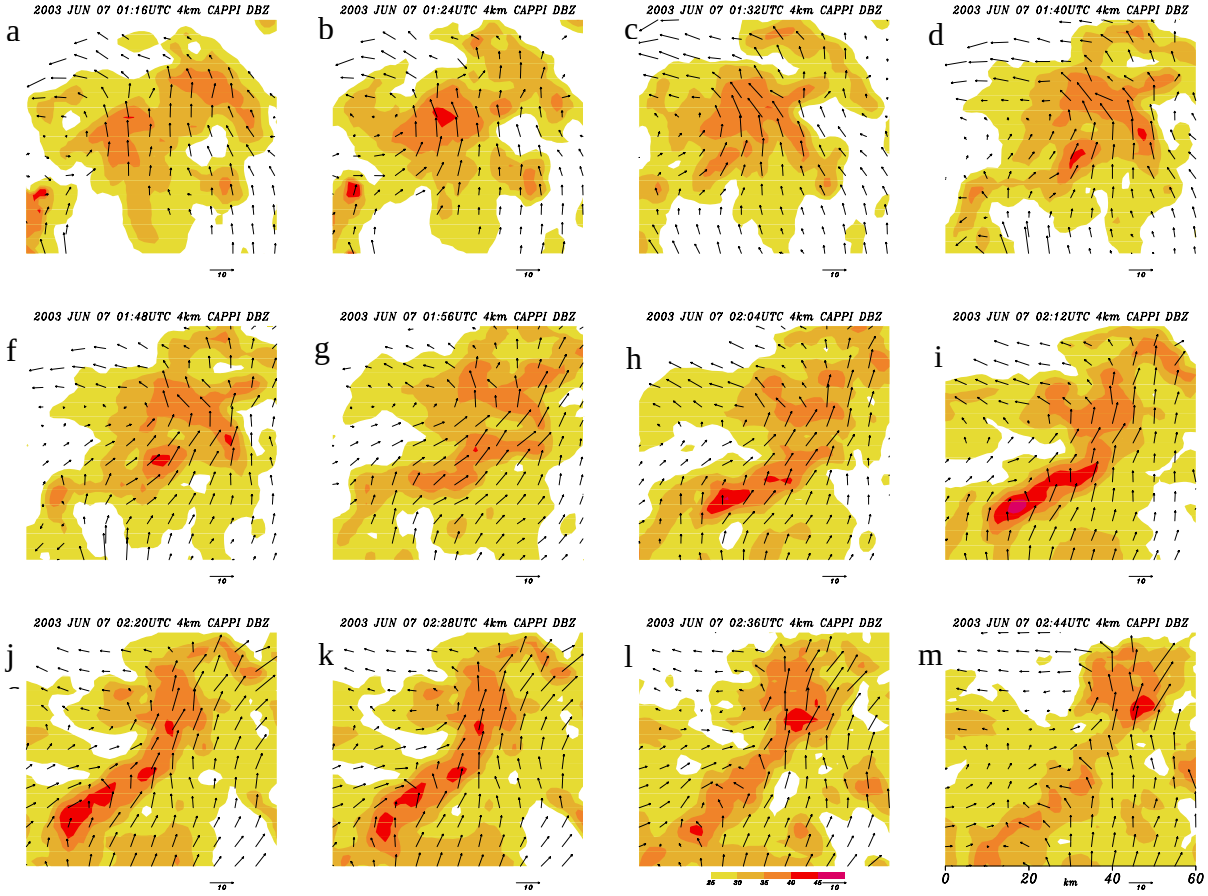

Fig. 3. Temporal sequence of reflectivity and synthesized wind field for northern bow segment from 0116 UTC to 0244 UTC 7 June 2003 (panel (a) to (m)) at 4 km level. The horizontal domain is 60 km X 60 km.

UTC 7 June (Fig. 2). An apparent wind shear line associated with a cyclonic circulation was located near the same position as surface front, extended from the surface to 700 hPa. The prefrontal southwesterly was strong with speed of 15 ms^{-1} at low levels. The horizontal temperature gradient (~1 ^{o}C per 100 km) was weak along the front,, indicating an imperceptible baroclinicity for both prefrontal and postfrontal area. The assessment of convective available potential energy (CAPE) from Makung sounding was 611 J kg^{-1}. Vertical wind shear was about 5 m s^{-1} (below level of 5 km). The bow-echo-type system occur in tropical environment (Jorgensen et al. 1997) had a CAPE of 1440 J kg^{-1} and vertical wind shear of 13 ms^{-1} at low level, which were not quite as severe as for midlatitude systems. However, the environmental condition of the present case was even weaker than that tropical system.

4. EVOLUTION OF ECHOES AND KINEMATIC FILED

Fig. 3 depicts the temporal sequence of composite echo and synthesized wind field for northern segment of LWEP at lower level. In the beginning (0116 UTC, Fig. 3a) a cyclonic circulation was located on the western flank of multi-cell. The cellular system organized to be a bow-shaped pattern between 0148 UTC (Fig. 3f) and 0156 (Fig. 3g) UTC, and the cyclonic circulation evolved to be a vortex located on the northern head of the system. By 0204 UTC (Fig. 3h), flow on the southern tip of system rotated clockwise, suggesting that an anticyclonic vortex was building up. Between 0204 and 0236 UTC (Fig. 3l) the flow pattern associated with system was characterized by cyclonic and anti-cyclonic vortexs on its northern and southern end, respectively, which were similar to the book-end vortices. The intense echo evolved into asymmetric segment; i.e., a comma-shaped echo, simultaneously. By 0236 UTC bow-shaped pattern disappeared and system revealed to be convective line instead. The cyclonic vortex still existed and propagated with northern end of comma echo. However, the anticyclonic one dissipated.

There was also a cyclonic vortex associated with southern segment of LEWP which exhibited rather bowing. The structural evolution of vortices could also be determined from time sequence (Fig. 4), though the wind field was incompletely deduced at certain time due to the restricted scanning area. By 0212 UTC (Fig. 4i), the vortex demonstrated an oval circulation. The intense echoes developed on its western and southeastern side. After 0244 UTC (Fig. 4m), the vortex tended to adjust its circulation being circular.

5. DISCUSSION

Some of features illustrated in the present case were more comparable with prior numerical modeling result presented by Weisman and Trapp (2003). The wave pattern of vortices resembled the combination of mesovortices Vh and Vi (Fig. 13 in their study). The flow pattern, distribution of vertical velocity and precipitation of southern cyclonic vortex (Fig. 5) were similar to vortex Vi as well, except that the magnitude of vertical velocity was much smaller and the horizontal scale was about three times larger.

The maximum vertical vorticity of the northern cyclonic vortex appeared first on the eastern side of vortex at 0156 UTC (Fig. 6g), the maximum value

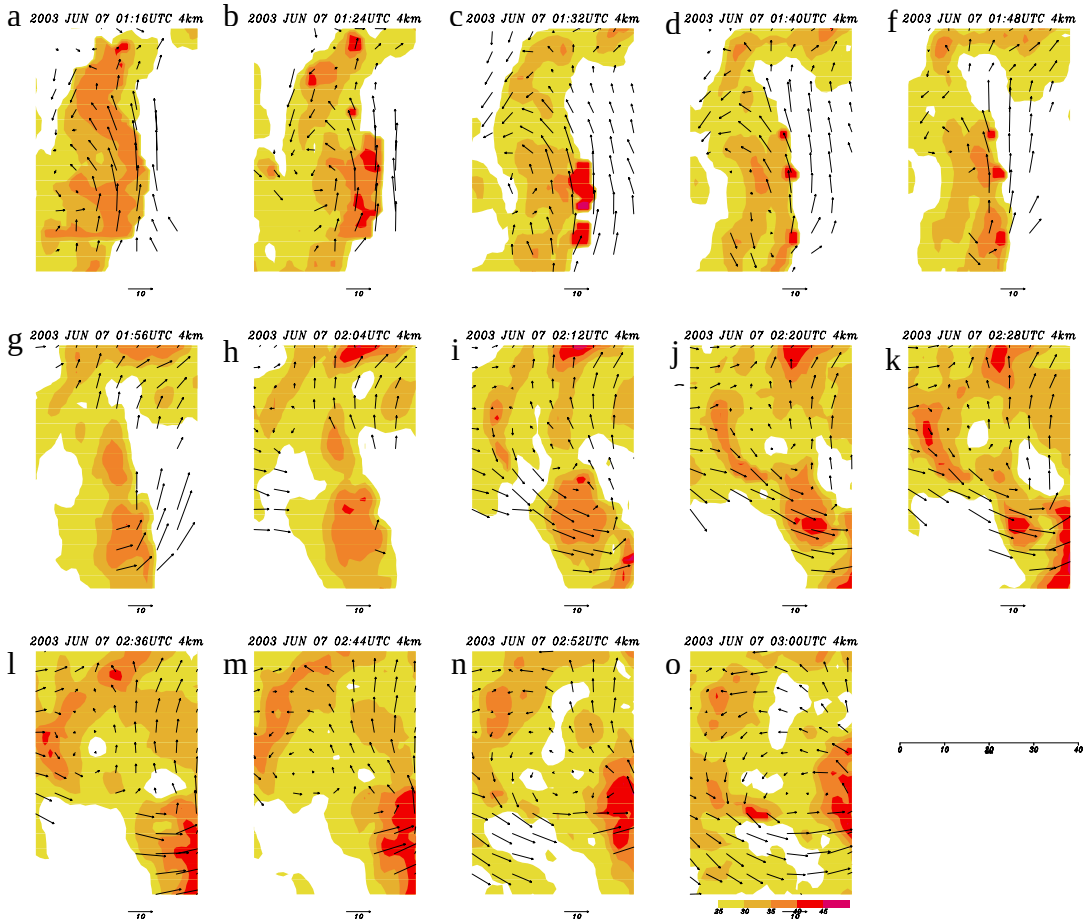

Fig. 4. Temporal sequence of reflectivity and synthesized wind field for southern cyclonic vortex from 0116 UTC to 0300 UTC 7 June 2003 (panel (a) to (o)) at 4 km level. The horizontal domain is 40 km X 60 km.

shifted westward and coincided with circulation center later on. The most intense one appeared at the level of 4 km, although the flow was curved rather than a closed circulation. Between 0156 and 0204 UTC (Fig. 6h), the maximum vorticity was obviously intensified (from 2 to 2.5 s^{-3}). The mechanism of vorticity change was examined from the tendency of vorticity equation. The vorticity tendency is computed after advecting two volumes of analyses to a common place. The local rate of change can be divided into four terms: horizontal advection, vertical advection, stretching and tilting. The result (Fig. 7) showed that stretching term dominated the tendency of relative vorticity which was near the core of maximum vorticity.

6. SUMMARY AND FUTURE STUDY

Dual-Doppler wind synthesis from operational radar network documented the evolutions of LEWP and book-end vortices which developed over the subtropical ocean in Asian area. The combinations of bow echo and vortices were similar to one of the simulated quasi-linear convective systems by Weisman and Trapp (2003), even though the environmental condition (CAPE

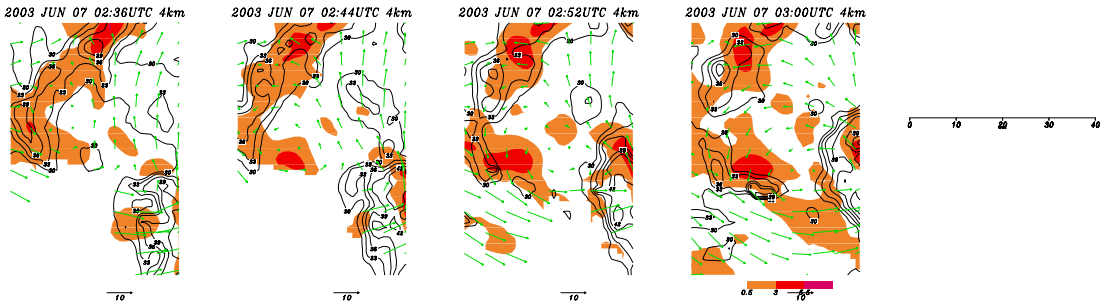

Fig. 5. The composite of Vertical velocity, reflectivity and synthesized wind field for southern cyclonic vortex from 0236 UTC to 0300 UTC 7 June 2003 at 4 km level. The shaded area represents vertical velocity. Contours stand for reflectivity. The horizontal domain is 40 km X 60 km.

and shear) of this case was much weaker. The northern bow-shaped convection resembled comma echo. This asymmetry became evident as the cyclonic vortex was more pronounced. A small anticyclonic vortex developed on the southern end of segment simultaneously. The vortex couplet was quite similar to the book-end vortices and more intense at 4 km level.

The flow pattern and distribution of vertical velocity around southern cyclonic vortex is also similar to the vortex of in Weisman's simulation. Their differences appeared on the magnitude of vertical velocity and horizontal scale.

The study is an ongoing research. A future attempt is to examine the pressure and buoyancy field in order to realize the contribution of these factors to the development of vortices.

REFERENCES

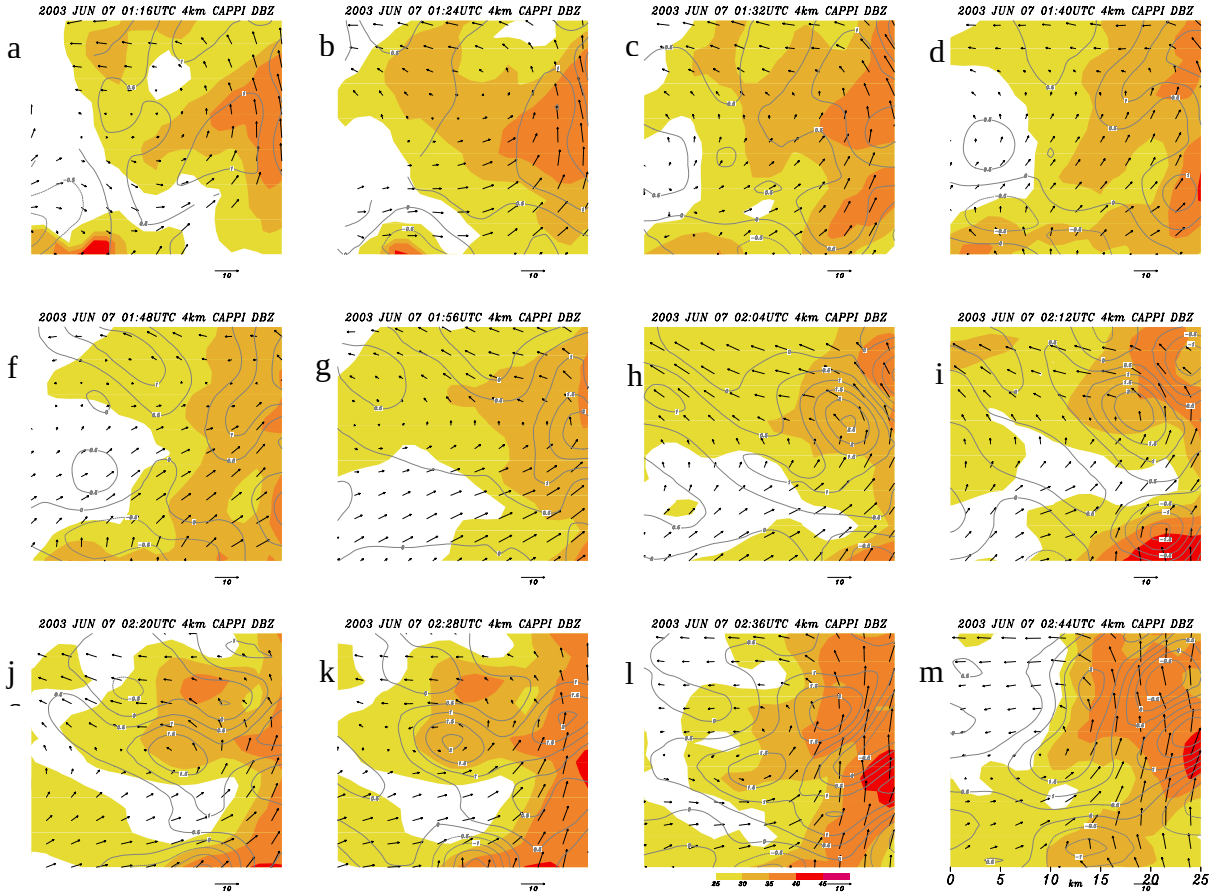

Fig. 6. Temporal sequence of veritcla relative vorticity, reflectivity and synthesized wind field for northern bow cyclonic vortex from 0116 UTC to 0244 UTC 7 June 2003 (panel (a) to (m)) at 4 km level. The shaded area represents reflectivity and contours stand for vertical vorticity. The horizontal domain is 25 km X 25 km.

Fujita, 1981: Tornadoes and downbursts in the context of generalized planetary scales. *J. Atmos. Sci.,* **38,** 1511–1524.

Jorgensen, D. P., M. A. LeMone and S. B. Trier, 1997: Structure and evolution of the 22 February 1993 TOGA COARE squall line: Aircraft observations of Precipitation, Circulation, and Surface Energy Fluxes. *J. Atmos. Sci.*: **54**, 1961–1985.

Mohr, C. G., L. J. Miller, R. L. Vaughan, and H. W. Frank, 1986: The merger of mesoscale datasets into a common Cartesian format for efficient and systematic analyses. *J. Atmos. Oceanic Technol.,* **3,** 143–161.

Oye, R., C. Mueller, and S. Smith, 1995: Software for radar translation, visualization, editing, and interpolation. Preprints, *27th Conf. on Radar Meteor.,* Vail, CO, Amer. Meteor. Soc., 359–361.

Skamarock, W. C., M. L. Weisman, and J. B. Klemp, 1994: Threedimensional evolution of simulated long-lived squall lines. *J. Atmos. Sci.,* **51,** 2563–2584.

Weisman, M. L., 1992: The role of convectively generated rearinflow jets in the evolution of long-lived mesoconvective systems. *J. Atmos. Sci.,* **49,** 1826–1847.

Weisman, and C. Davis, 1998: Mechanisms for the generation of mesoscale vortices within quasi-linear convective systems. *J. Atmos. Sci.,* **55,** 2603–2622.

Weisman, M. L. and R. J. Trapp, 2003: Low-Level Mesovortices within Squall Lines and Bow Echoes. Part I: Overview and Dependence on Environmental Shear. *Mon. Wea. Rev.*: **131**, 2779–2803.

Davis, C., N. Atkins, D. Bartels, L. Bosart, M. Coniglio, G. Bryan, W. Cotton, D. Dowell, B. Jewett, R. Johns, D. Jorgensen, J. Knievel, K. Knupp, W.-C. Lee, G. Mcfarquhar, J. Moore, R. Przybylinski, R. Rauber, B. Smull, R. Trapp, S. Trier, R. Wakimoto, M. Weisman and C. Ziegler, 2004: The Bow Echo and MCV Experiment: Observations and Opportunities. *Bulletin of the American Meteorological Society*: **85**, 1075-1093.

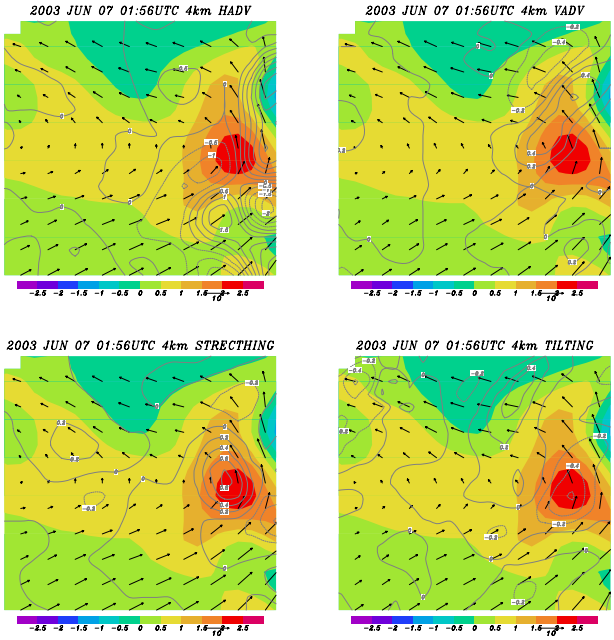

Fig. 7. The contribution of horizontal (HADV), vertical (VADV) advection, stretching and tilting term (contour) to vorticity tendency for northern vortice. The shaded area represents vertical vorticity.